[3] a) T. Kawashima, T. Soda, K. Kato, R. Okazaki, *Phosphorus Sulfur Silicon* **1996**, *109–110*, 489–492; b) T. Kawashima, T. Soda, R. Okazaki, *Angew. Chem.* **1996**, *108*, 1206–1208; *Angew. Chem. Int. Ed. Engl.* **1996**, *35*, 1096–1098; c) N. V. Timosheva, T. K. Prakasha, A. Chandrasekaran, R. O. Day, R. R. Holmes, *Inorg. Chem.* **1995**, *34*, 4525–4526; d) N. V. Timosheva, A. Chandrasekaran, T. K. Prakasha, R. O. Day, R. R. Holmes, *Inorg. Chem.* **1996**, *35*, 6552–6560; e) S. Kumaraswamy, C. Muthiah, K. C. Kumara Swamy, *J. Am. Chem. Soc.* **2000**, *122*, 964–965.

[4] O. Lösking, H. Willner, H. Oberhammer, J. Grobe, D. L. Van, *Inorg. Chem.* **1992**, *31*, 3423–3427.

[5] a) K. Kajiyama, M. Yoshimune, M. Nakamoto, S. Matsukawa, S. Kojima, K.-y. Akiba, *Org. Lett.* **2001**, *3*, 1873–1875; b) S. Kojima, K. Kajiyama, M. Nakamoto, K.-y. Akiba, *J. Am. Chem. Soc.* **1996**, *118*, 12866–12867; c) K. Kajiyama, S. Kojima, K.-y. Akiba, *Tetrahedron Lett.* **1996**, *37*, 8409–8412.

[6] S. Matsukawa, S. Kojima, K. Kajiyama, Y. Yamamoto, K.-y. Akiba, S. Re, S. Nagase, *J. Am. Chem. Soc.* **2002**, *124*, in press.

[7] R. S. Berry, *J. Chem. Phys.* **1960**, *32*, 933–938.

$$\mathbf{1bA} \xrightarrow{\Psi_{Et}} \xrightarrow{\Psi_{Me}} \mathbf{1bB}$$

[8] R. M. Moriarty, J. Hiratake, K. Liu, A. Wendler, A. K. Awasthi, R. Gilardi, *J. Am. Chem. Soc.* **1991**, *113*, 9374–9375.

[9] Spectroscopic data and ORTEP drawings are in the Supporting Information. Synthesis and complete characterization of the compounds will be reported in due course.

[10] S. Berger, S. Braun, H.-O. Kalinowski, *NMR Spectroscopy of the Non-Metallic Elements*, Wiley, Chichester, **1997**, p. 900.

[11] M. Charton, *Prog. Phys. Org. Chem.* **1981**, *13*, 119–251.

[12] R. W. Taft, Jr., *Steric Effects in Organic Chemistry* (Ed.: M. S. Newman), Wiley, New York, **1956**, p. 598.

[13] S. A. Bone, S. Trippett, P. J. Whittle, *J. Chem. Soc. Perkin Trans. 1* **1977**, 437–438.

[14] C. Reichardt, *Solvents and Solvent Effects in Organic Chemistry*, VCH, Weinheim, **1988**, pp. 407–411.

[15] CCDC-192716 (**1b**) and CCDC-153789 (**1h**) contain the supplementary crystallographic data for this paper. These data can be obtained free of charge via www.ccdc.cam.ac.uk/conts/retrieving.html (or from the Cambridge Crystallographic Data Centre, 12 Union Road, Cambridge CB2 1EZ, UK; fax: (+44) 1223-336-033; or deposit @ccdc.cam.ac.uk). Crystals suitable for X-ray structure determination were mounted on a Mac Science DIP2030 imaging plate equipped with graphite-monochromated $Mo_{K\alpha}$ radiation ($\lambda = 0.71073$ Å). Unit cell parameters were determined by autoindexing several images in each data set separately with program DENZO.[16] For each data set, rotation images were collected in 3° increments with a total rotation of 180° about ϕ. Data were processed by using SCALEPACK.[16] The structure was solved using the teXsan (Rigaku) system and refined by the full-matrix least-squares method. Crystal data for **1b**: monoclinic system, space group $P2_1/n$ (no. 14), $a = 10.4300(2)$, $b = 18.0140(4)$, $c = 12.4740(3)$ Å, $\beta = 102.795(1)°$, $V = 2285.49(9)$ Å^3, $Z = 4$, $\rho_{calc} = 1.628$ g cm^{-3}. $R = 0.0650$ ($Rw = 0.1453$) for 4749 observed reflections (325 parameters) with $I > 3\sigma(I)$. Goodness of fit = 1.362. Selected bond lengths [Å]: P(1)-O(1) 2.120(2), P(1)-C(1) 1.824(3), P(1)-C(10) 1.849(3), P(1)-C(19) 1.855(3), P(1)-C(20) 1.838(3). **1h**: triclinic system, space group $P\bar{1}$ (no. 2), $a = 11.7550(4)$, $b = 12.5610(8)$, $c = 18.904(1)$ Å, $\alpha = 93.532(2)$, $\beta = 102.047(3)$, $\gamma = 100.279(4)°$, $V = 2671.8(2)$ Å^3, $Z = 4$, $\rho_{calc} = 1.547$ g cm^{-3}. $R = 0.0658$ ($Rw = 0.1320$) for 7190 observed reflections (740 parameters) with $I > 3\sigma(I)$. Goodness of fit = 1.767. Selected bond lengths [Å], **1hA**: P(1)-O(1) 2.078(3), P(1)-C(1) 1.809(5), P(1)-C(10) 1.850(4), P(1)-C(19) 1.853(5), P(1)-C(20) 1.865(4); **1hB**: P(2)-O(3) 2.043(3), P(2)-C(27) 1.844(5), P(2)-C(36) 1.858(4), P(2)-C(45) 1.892(5), P(2)-C(52) 1.819(5).

[16] Z. Otwinowski, University of Texas, Southwestern Medical Center.

Preferential Location of Ge Atoms in Polymorph C of Beta Zeolite (ITQ-17) and Their Structure-Directing Effect: A Computational, XRD, and NMR Spectroscopic Study**

German Sastre, Jose A. Vidal-Moya, Teresa Blasco, Jordi Rius, Jose L. Jordá, Maria T. Navarro, Fernando Rey, and Avelino Corma*

Zeolites are crystalline aluminosilicates with a regular array of microporous systems which are responsible for the outstanding properties of these materials in adsorption, ion exchange, and catalysis.[1–3] Since most of these properties strongly depend on pore dimensions and topology, there is an incentive to develop tailor-made syntheses of zeolites. Although improvements in the understanding of zeolite synthesis have been made through the rational design of organic structure-directing agents (SDAs),[4] the predictable synthesis of the desired structures is far from being achieved, this is because of the large number of parameters that influence the reactions.

We recently showed that the rate of nucleation of zeolite ITQ-7, a zeolite containing double four-member rings (D4Rs), is strongly accelerated when Ge atoms are introduced into the framework.[5] Furthermore, by means of ^{19}F and ^{29}Si MAS NMR (MAS = magic-angle spinning) spectroscopy we indirectly postulated that the Ge atoms were preferentially occupying framework positions at the D4R units.[6] These observations made us think that the introduction of Ge atoms could direct the synthesis of zeolites towards structures containing D4Rs as secondary building units (SBUs), which are rare.[7] Our first attempt was directed to the synthesis of the previously elusive pure polymorph C of Beta zeolite, which contains D4Rs (with the International Zeolite Associ-

[*] Prof. A. Corma, Dr. G. Sastre, J. A. Vidal-Moya, Dr. T. Blasco, Dr. M. T. Navarro, Dr. F. Rey
Instituto de Tecnologia Química, (UPV-CSIC)
Universidad Politecnica de Valencia
Avenida Los Naranjos s/n, 46022 Valencia (Spain)
Fax: (+34) 96-387-7809
E-mail: acorma@itq.upv.es
Dr. J. Rius, Dr. J. L. Jordá
Institut de Ciencia de Materials de Barcelona (CSIC)
Campus de la UAB, 08193 Bellaterra, Catalunya (Spain)

[**] We thank Generalitat Valenciana (project GV01-492) and Spanish CICYT (projects MAT 2000-1392, MAT 2000-1167-C02-01, and PB98-0483) for financial support, and C^4 (Centre de Computacio i Comunicacions de Catalunya) and Centro de Cálculo de la Universidad Politécnica de Valencia for the use of their computational facilities. The High Performance Computational Chemistry Group from Pacific Northwest National Laboratory (Richland, Washington 993520999), is acknowledged for making available NWChem version 4.0, a computational chemistry package for parallel computers. The authors also acknowledge financial support from EEC ARI contract HPRI-CT-1999-00042 to access the HRSHTLNMR facility. We also thank Dr. L. Delevoye from Bruker Biospin for recording some NMR spectra. J.L.J. thanks UPV for a postdoctoral grant. J.A.V.M. acknowledges Bruker (Program I3P) for a predoctoral grant.

Supporting information for this article is available on the WWW under http://www.angewandte.org or from the author.

  0044-8249/02/4124-4722 $ 20.00+.50/0

ation code BEC[7a]). The silicon-free Ge material with BEC structure (named FOS-5[7b]) was first isolated from a ASU-9 and FOS-5 mixture. Later, a pure phase was obtained as a silicogermanate (ITQ-17[8]). We showed that pure polymorph C of Beta zeolite could be synthesized with a large variety of organic SDAs when Si atoms were partially substituted by Ge atoms,[8] regardless of whether F^- or OH^- ions were used as mineralizing agents.[8b] The synthesis of pure polymorph C of Beta zeolite represents a unique opportunity to prove the preferential occupation of Ge atoms in the D4Rs. Indeed, as ITQ-17 is a pure structure, XRD techniques can be used to unequivocally ascertain whether Ge tends to locate in the positions of the D4Rs.

Herein we report a complete study of ITQ-17 zeolite with different Si:Ge ratios by means of: a) computational chemistry techniques based on force-field methods and lattice-energy minimization, b) XRD and electron density studies, and c) ^{19}F MAS NMR spectroscopy. All these techniques point to the preferential siting of Ge at the D4R until four Ge atoms are present in these SBUs. As the Ge content increases, other sites start to become occupied preferentially to avoid the formation of Ge–O–Ge bonds in D4Rs, which would decrease the stability of the system.

The syntheses of Ge-containing ITQ-17 samples were performed by using a modified literature method (see Supporting Information).[8a]

The chemical composition and the main properties of the samples studied are summarized in Table 1. Pure polymorph C of the Beta intergrowth (BEC structure) is the only phase obtained in the whole range of Si:Ge ratios used. In contrast, when Ge is not present, ITQ-4 or Beta zeolites are produced. The directing effect of the Ge atoms is also reflected by the increasing crystallization time needed to obtain completely crystalline ITQ-17 zeolite when the Ge content in the synthesis gel is decreased.

Since the Ge atoms enter the BEC framework during the synthesis, the calculation of the stability of the different sites (Figure 1) must take into consideration the interaction of the SDA and fluoride species with the framework (the general unit cell composition is $Ge_xSi_{32-x}O_{64}F_2BD_2$; BD = the 1-benzyl-4-aza-1-azoniacyclo[2,2,2]octane cation).

The positions of the two fluoride anions can be safely placed at the two existing D4R cages per unit cell of the BEC structure by means of NMR spectroscopic techniques.

The orientation of the two BD^+ molecules was optimized by searching for the minimum energy configuration on the pure silica structure. Computational details are provided as Supporting Information.

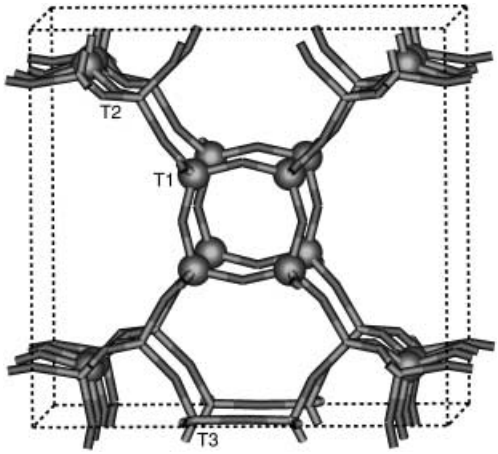

Figure 1. Crystallographic structure of ITQ-17 showing the three different T sites. T1 positions are at the D4Rs. T2 positions are connecting D4Rs, and T3 positions are part of single four-rings. Three interconnected straight 12 membered ring channels are present, the dimensions of which are: 5.9 × 6.5 Å (parallel to [100] and [010]) and 6.3 × 6.3 Å (parallel to [001]).

One Ge atom was alternatively placed at different T sites of the unit cell and the resultant systems were optimized again. The stability of the Ge-substituted frameworks was then calculated (Table 2). The Ge-atom incorporation in site T1 is the most favorable in the presence of SDA and F species. The Ge1 position appears more favored with respect to Ge2 and Ge3 by 44.3 and 58.0 kJ mol^{-1}, respectively. This points to a preferential location of the Ge atoms in the T1 sites, and to similar occupations of Ge at the T2 and T3 sites.

Table 2. Excerpt of the geometry analysis[20] of the calculated Ge-ITQ-17 with one Ge per unit formula, and including the template ($Ge_1Si_{31}O_{64}F_2BD_2$). The Ge atom is alternatively introduced in sites T1, T2, and T3.

	Ge in T1		Ge in T2		Ge in T3	
T-label	T-O-T [°]	T–O [Å]	T-O-T [°]	T–O [Å]	T-O-T [°]	T–O [Å]
Si1	138.1	1.623	138.1	1.625	138.2	1.625
Ge1	132.6	1.745	–	–	–	–
Si2	146.9	1.606	147.1	1.606	146.9	1.606
Ge2	–	–	142.5	1.715	–	–
Si3	154.7	1.598	154.4	1.597	155.2	1.597
Ge3	–	–	–	–	150.6	1.707

It is interesting to calculate the possible distributions of Ge for a composition within the samples of ITQ-17 synthesized in this work. The selected unit-cell composition was $Ge_{12}Si_{20}O_{64}F_2BD_2$. Again, all the atoms of the system, as well as

Table 1. Chemical compositions and main characterization results of Ge containing ITQ-17 samples.

Sample	Chemical composition [mol/unit cell]				Si:Ge ratio	Unit cell volume	Micropore volume	Crystallinity [%][b]
	Si	Ge	SDA	F	[Å^3/unit cell]		[cm^3 mol$_{TO2}^{-1}$][a]	
17 Ge[c]	14.80	17.20	2.96	1.74	0.9:1	2215	14.8	100
11 Ge[d]	20.57	11.43	2.68	1.95	1.8:1	2194	15.6	106
7 Ge[d]	24.87	7.13	2.32	1.58	3.5:1	2167	13.4	90
6 Ge[d]	26.05	5.95	2.53	1.19	4.4:1	2144	14.2	96
4 Ge[d]	28.08	3.92	2.00	n.d.	7.2:1	2145	12.0	81

[a] Calculated from the micropore volume determined by applying the t-plot method to the adsorption branch of the N_2 isotherm. [b] With respect to sample 17 Ge. [c] Synthesized using tetramethylammonium cations as SDA. [d] Synthesized using 1-benzyl-4-aza-1-azoniacyclo [2,2,2,] octane cations as SDA.

  0044-8249/02/4124-4723 $ 20.00+.50/0

the cell parameters, were allowed to relax during the optimizations. Although the most stable distribution of the twelve Ge atoms in the unit cell is unknown, it may be assumed that a) site T1 will be the most populated and b) the Ge occupations at T2 and T3 are similar. Therefore, the starting Ge occupations of eight Ge1, two Ge2, two Ge3 were proposed, so that eight T1, two T2, and two T3 positions were occupied by Ge atoms. Since the total number of sites is sixteen T1, eight T2, eight T3, there are many possible distributions. We checked a sampling of 100 random configurations with eight Ge1, two Ge2, two Ge3 and the final optimized energies are shown in Figure 2. From the analysis of these data it is difficult to extract trends which explain what makes one configuration more stable than another in terms of a single variable.

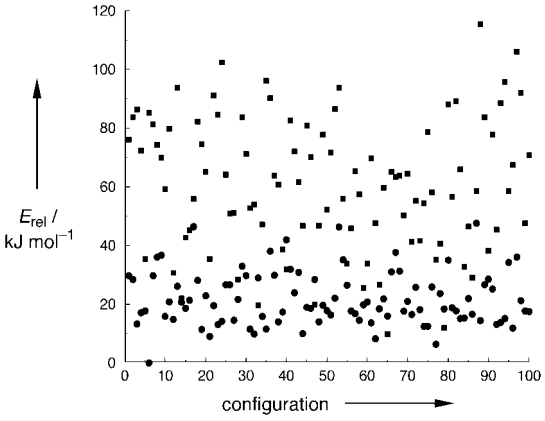

Figure 2. Plot of the energetic stability of 100 random configurations generated in the $Ge_{12}Si_{20}O_{64}F_2BD_2$ unit cell with eight Ge in T1 sites, two Ge in T2 sites, and two Ge in T3 sites (■); and with eight Ge in opposite corners of D4Rs, two Ge in T2 sites and two Ge in T3 sites (●).

The next step was to place eight Ge1 atoms in opposite corners of the two D4Rs since, because of their higher symmetry, this may induce low energy configurations. As in the previous case, the two Ge2 and two Ge3 atoms were distributed randomly among the corresponding eight T2 and eight T3 sites, respectively. 100 Random configurations were generated and the final minimized energies are plotted in Figure 2. It can be seen that most of these new 100 configurations are more stable than the previous 100 configurations. These computational calculations allow us to conclude that, in the presence of SDAs, the substitution of Si atoms by Ge atoms at the T1 site is energetically favored, and that at Si:Ge≅1.67:1, configurations with Ge at the opposite sites of a D4R are preferred to avoid formation of Ge–O–Ge bonds.

Calculations with five Ge1, one Ge2, and one Ge3 in the unit cell have also been performed ($Ge_7Si_{25}O_{64}F_2BD_2$ that is, Si:Ge≅3.5:1). Several distributions of a total of five Ge atoms among the two D4Rs (T1 sites) have been tested: a) three and two Ge atoms; b) four and one Ge atom(s), and finally, c) five and no Ge atoms. 100 Random configurations were generated and optimized for each starting distribution (Figure 3). It can be seen that the configurations with five Ge atoms in one D4R are clearly higher in energy, and consequently less probable

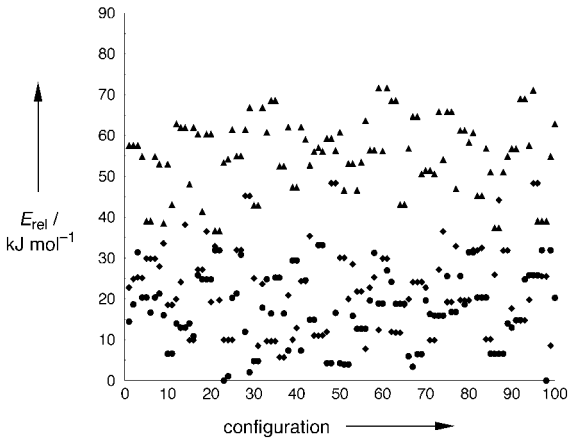

Figure 3. Plot of the energetic stability of 100 random configurations generated in the $Ge_7Si_{25}O_{64}F_2BD_2$ unit cell with: five Ge in T1 sites, one Ge in T2 sites, and one Ge in T3 sites. The five Ge in the two D4R (T1 sites) present in the unit cell have been distributed: three Ge in a D4R and two Ge in the other D4R (●), four Ge and one Ge (◆), and five Ge and zero Ge (▲).

than the configurations with three or four Ge atoms in each D4R.

The indexing of the XRD patterns of the calcined Ge-ITQ-17 samples and the subsequent analysis of the systematic absences confirm that all the samples belong to space group $P4_2/mmc$ (no. 131), that is, the space group is independent from the isomorphic replacement of Si atoms by Ge atoms. The corresponding Rietveld refinements were carried out starting from the previously reported structure of polymorph C[8] in which Si atoms had been partially substituted with Ge atoms.

As expected from its larger ionic radii, an increase in the Ge content produces a lengthening of the cell parameters and consequently an increase in the cell volume (Table 1), indicating that the Ge atoms replace the Si atoms isomorphically in the BEC stucture.

Additionally, the Ge distribution among the three different T sites of the BEC structure can be derived from the refinement of the respective scattering powers.

However, prior to any further discussion it is worth studying the stability of Ge atoms placed in framework positions upon calcination by comparing the Ge-atom distribution among the different crystallographic sites of a particular ITQ-17 sample (11 Ge) before and after calcination (see Supporting Information). No important differences in the Ge distribution are observed between the untreated ITQ-17 sample and the corresponding calcined ITQ-17 material, which indicates that the Ge atoms essentially remain in the framework, and at the same crystallographic sites upon calcination. Consequently, XRD analyses on the calcined materials can be safely performed.

The relative distribution of Ge atoms in these sites as a function of the total Ge content in the calcined ITQ-17 sample is given in Figure 4. The graphic shows that for a Ge content of less than approximately eight Ge atoms per unit cell (that is, Ge:(Si + Ge) ≈ 1:4), the Ge population grows more steeply at site T1 than at sites T2 and T3 which indicates the preferential incorporation of the Ge atoms in the D4R units. However, the

  0044-8249/02/4124-4724 $ 20.00+.50/0

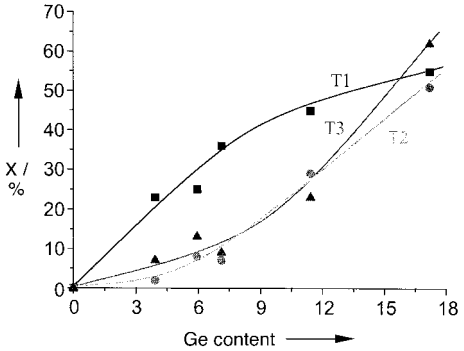

Figure 4. Relative Ge occupation in the different T sites of the polymorph C of the Beta zeolite as a function of the Ge content (number of Ge atoms per unit cell) of the ITQ-17.

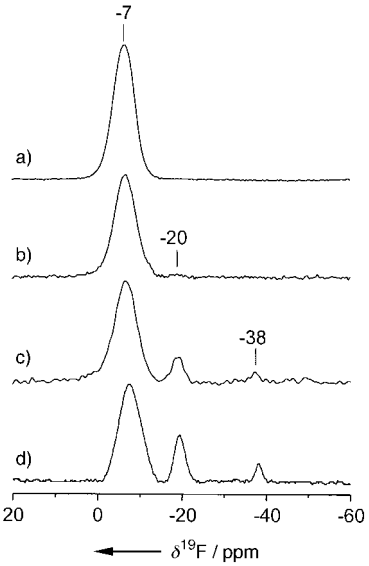

Figure 5. ^{19}F MAS NMR spectra of ITQ-17 at different Ge contents: a) 17 Ge, Si:Ge = 0.8:1; b) 11 Ge, Si:Ge = 1.8:1; c) 7 Ge, Si:Ge = 3.5:1; d) 4 Ge, Si:Ge = 7.2:1.

populations at T2 and T3 sites rise faster than for T1 when the Ge content is further increased.

Finally, it is interesting to calculate the evolution of the mean T1–O bond length in a D4R unit, for the sample Si:Ge = 0.9:1 it is 1.70(1) Å. For the rest of studied samples, the average oscillates between 1.67 and 1.68(1) Å. This small variation indicates a fast and selective filling of this site.

On the other hand, T2–O and T3–O bond lengths for the low-Ge-content samples correspond to that obtained for a typical Si–O bond that is, 1.62(1) Å, as expected from their low Ge occupancy at these positions. However, for the sample with a Si:Ge ratio of 0.9:1 (17 Ge), where a high replacement of Si atoms with Ge atoms takes place, these T–O bond lengths increase up to a value of 1.70(1) Å, as found for the T1 site.

The analysis of the XRD data clearly shows that, for low Ge contents, the incorporation of Ge atoms occurs preferentially at the T1 sites in the D4R units, with up to a 50% replacement. However, as soon as this value is reached, the two remaining T sites (T2 and T3) start to be preferentially occupied by Ge atoms. The XRD data gives information on the overall substitution of Ge atoms at T1 sites, but not about the distribution of the hetero atoms among the D4R cages. ^{19}F MAS NMR spectroscopy is very sensitive to the F^--ion environment and provides evidence for the heterogeneous nature of the D4R composition of Ge-ITQ-7.[6] Figure 5 shows the ^{19}F MAS NMR spectra of four Ge-ITQ-17 samples with different Ge contents. For sample 4 Ge (Si:Ge = 7.1:1), the spectrum consists of a relatively weak signal at $\delta = -38$ ppm typical of F^- ions located in pure siliceous D4R cages,[9,10] and two more resonance signals at $\delta = -20$ and -7 ppm. According to previous results for Ge-ITQ-7, the incorporation of Ge into the D4R sites can be estimated from the relative intensity of the ^{19}F resonance signals.[6] Assuming that the signal at $\delta = -20$ ppm is produced by F[7Si 1Ge] sites,[6] the assignment of the signal at $\delta = -7$ ppm to F[5Si 3Ge] or to F[4Si 4Ge] leads to site occupancies of 30% or 40%, respectively, the former having a better agreement with the XRD results (23% Ge at site T1).

For the samples with higher Ge content, 11 Ge and 17 Ge (Si:Ge = 1.8:1 and 0.9:1), the corresponding ^{19}F spectra only contain one resonance signal at $\delta = -7$ ppm, although some residual intensity at $\delta = -20$ ppm remains for the former. For these two samples, the Rietveld refinements yield around 50% Ge occupancy at site T1, so that the signal at $\delta = -7$ ppm in the ^{19}F NMR spectrum should be assigned to a fluoride ion in a D4R formed by four SiO_4 and four GeO_4 tetrahedra; that is, F[4Si, 4Ge].

Although the complete interpretation of the ^{19}F NMR spectra is not definitive, the results are consistent with those derived from the analysis of the XRD data. The downfield resonance signals in the ^{19}F NMR spectrum increase with the Ge content, and for Ge-rich samples 11 Ge and 17 Ge (Figure 5) almost the only spectral feature is the downfield signal.

In conclusion, these results suggest that in the ITQ-17 zeolite, Ge is being progressively incorporated into a D4R to reach four (or three) Ge atoms per cage, and then a further increase of the Ge content favors the substitution of Si atoms at crystallographic sites other than T1 at the D4R. In light of our previous results[5] and those presented here, it is possible to predict the formation of new zeolite structures containing D4R SBUs by introducing the directing effect of the Ge atoms.[11]

Experimental Section

XRD: The XRD measurements were carried out in an X'Pert diffractometer provided with a secondary graphite monochromator. In situ calcination of the prepared samples and the subsequent XRD measurements were performed as described in the Supporting Information. Inspection of the diffraction patterns indicates no significant amorphous material except for the sample prepared with the highest Si:Ge ratio.

Rietveld Refinement: The space-group symmetry of the calcined samples was first checked with the whole-profile fitting program AJUST.[12] The subsequent Rietveld refinements with the program FULLPROF 98[13] were performed using the 2Θ range from 5 to 70° with two excluded regions, 38.76°–40.76° and 45.24°–47.24°, because of the presence of the (111) and (200) diffraction peaks of the Pt sample holder. Eight profile parameters (including cell parameters and zero shift) and 25 structural parameters were refined using a pseudo-Voigt function with a visually estimated background. The Ge distribution among the different T sites was derived

  0044-8249/02/4124-4725 $ 20.00+.50/0

from the refined effective number of electrons at each T site by taking advantage of the high contrast between the scattering powers of Si and Ge.

Solid state NMR spectroscopy: The spectra were recorded under magic angle spinning (MAS) at room temperature. ^{19}F spectra were was measured in a Bruker Av-400 spectrometer at 376.8 MHz in 2.5 mm diameter zirconia rotors at spinning rate of 30 kHz. The ^{19}F spectra were collected using pulses of 3 μs corresponding to a magnetization flip angle of π/2 rad and a recycle delay of 100 s to ensure the complete recovery of the magnetization. The ^{19}F spectra were referred to $CFCl_3$.

Computational chemistry: methodology and model. All calculations were performed using lattice-energy minimization techniques and the GULP code,[14] employing the Ewald method for summation of the long-range Coulombic interactions, and direct summation of the short-range interactions with a cutoff distance of 12 Å. The RFO (rational function optimiser) technique was used as the cell minimization scheme with a convergence criterion of a gradient norm below 0.001 eV Å^{-1}. The empirical shell model forcefield for zeolites[15] was used throughout, with the inclusion of the forcefields for Ge[16] and F[17] atoms. The force-fields by Kiselev et al.,[18] and by Oie et al.[19] were used for the SDA–zeolite and SDA–SDA interactions, respectively. In the organic SDA, the charge distribution has been obtained by means of the quantum chemistry Hartree–Fock method by using a 6-31G** basis set and the calculations have been performed by means of the NWCHEM package.

Received: May 22, 2002
Revised: September 24, 2002 [Z19356]

[1] J. A. Rabo, P. H. Kasai, *Prog. Solid State Chem.* **1975**, *9*, 1.
[2] D. Barthomeuf, *J. Phys. Chem.* **1979**, *83*, 249.
[3] P. A. Jacobs, *Catal. Rev. Sci. Eng.* **1982**, *24*, 415.
[4] R. F. Lobo, S. I. Zones, M. E. Davis, *J. Inclusion Phenom. Mol. Recognit. Chem.* **1995**, *21*, 47.
[5] A. Corma, M. J. Díaz-Cabañas, V. Fornés, *Angew. Chem.* **2000**, *112*, 2436; *Angew. Chem. Int. Ed.* **2000**, *39*, 2346.
[6] T. Blasco, A. Corma, M. J. Diaz-Cabañas, F. Rey, J. A. Vidal-Moya, C. M. Zicovich-Wilson, *J. Phys. Chem. B* **2002**, *106*, 2634.
[7] a) C. Baerlocher, W. M. Meier, D. H. Olson, *Atlas of Zeolite Framework Types*. 5th revised edition, Elsevier, Amsterdam, **2001**. Also in http://www.iza-structure.org/; b) T. Conradsson, M. S. Dadachov, X. D. Zou, *Microporous Mesoporous Mater.* **2000**, *41*, 183.
[8] a) A. Corma, M. T. Navarro, F. Rey, J. Rius, S. Valencia, *Angew. Chem.* **2001**, *113*, 2337; *Angew. Chem. Int. Ed.* **2001**, *40*, 2277; b) A. Corma, M. T. Navarro, F. Rey, S. Valencia, *Chem. Commun.* **2001**, 1486.
[9] P. Caullet, J. L. Guth, J. Hazm, J. M. Lamblin, *Eur. J. Solid State Inorg. Chem.* **1991**, *28*, 359.
[10] L. A. Villaescusa, P. A. Barrett, M. A. Camblor, *Angew. Chem.* **1999**, *111*, 2164; *Angew. Chem. Int. Ed.* **1999**, *38*, 1997.
[11] A. Corma, M. J. Díaz-Cabañas, J. Martínez-Triguero, F. Rey, J. Rius, *Nature* **2002**, *418*, 514.
[12] J. Rius, J. L. Jordá, AJUST/01, Institut de Ciència de Materials de Barcelona (CSIC).
[13] J. Rodríguez-Carvajal, T. Roisnel, FULLPROF 98 and WinPLOTR: New Windows 95/NT Applications for Diffraction Commission For Powder Diffraction, International Union for Crystallography, Newletter No. 20 (May-August) **1998**.
[14] J. D. Gale, *J. Chem. Soc. Faraday Trans.* **1997**, *93*, 629.
[15] R. A. Jackson, C. R. A. Catlow, *Mol. Simul.* **1988**, *1*, 207.
[16] G. Sastre, J. D. Gale, *Chem. Mater.*, submitted.
[17] A. R. George, C. R. A. Catlow, *Zeolites* **1997**, *18*, 67.
[18] A. V. Kiselev, A. A. Lopatkin, A. A. Shulga, *Zeolites* **1985**, *5*, 261.
[19] T. Oie, T. M. Maggiora, R. E. Christoffersen, D. J. Duchamp, *Int. J. Quantum Chem. Quantum Biol. Symp.* **1981**, *8*, 1.
[20] G. Sastre, J. D. Gale, *Microporous Mesoporous Mater.* **2001**, *43*, 27.

Solid-State NMR Studies of MCM-41 Supported with a Highly Catalytically Active Cluster**

Matthew D. Jones, Melinda J. Duer,*
Sophie Hermans, Yaroslav Z. Khimyak,
Brian F. G. Johnson, and John Meurig Thomas

In 1992, Beck et al.[1] reported the first synthesis of a new classification of silicate/aluminosilicate materials. The topic of this work, MCM-41, is one such member of this extensive family of mesoporous materials.[1] The high surface area, typically up to 1000 $m^2 g^{-1}$, and the high concentration of silanol groups has led to the exploitation of this material as a support for anchored catalysts, in particular the highly promising catalysts derived from bimetallic clusters.[2,3] Bimetallic nanoparticles are becoming increasingly important in modern heterogeneous catalysis,[4] because of enhanced catalytic activity arising from the synergetic effects between the two metallic moieties. Further enhancement of activity is brought about by the small size of the particles. Recently, highly effective hydrogenation catalysts based on bimetallic clusters encapsulated in the channels of MCM-41 have been developed.[3,5–7] For example, the nanocatalyst derived from the cluster $[Pd_6Ru_6(CO)_{24}][NEt_4]_2$ is highly effective in the conversion of naphthalene to *cis*-decalin under mild conditions.[7] The formation of these nanocatalysts involves first the deposition of the anionic cluster within the pores of MCM-41 followed by removal of CO ligands, which produces the supported "naked" nanoparticles. Significantly, we have been able to establish, by FT-IR and EXAFS spectroscopy, that the structural motif of the cluster is maintained in the mesopore.[7,8] The further development of these very important catalytic systems depends crucially on understanding how the clusters are supported in the mesopore. We have recently completed a study which demonstrates the importance of the counterion in the binding process. We show that the counterion is intrinsically linked to the walls of the mesopore, acting like a molecular "glue" binding the cluster.

In particular we have studied the interactions between the surface of MCM-41 and the highly effective catalyst derived from the $[Pd_6Ru_6(CO)_{24}][NEt_4]_2$ cluster, by solid-state NMR spectroscopy. We have used $^{29}Si\{^1H\}$ cross polarization (CP)

[*] Dr. M. J. Duer, M. D. Jones, Dr. S. Hermans, Dr. Y. Z. Khimyak, Prof. B. F. G. Johnson
Department of Chemistry
University of Cambridge
Lensfield Road, Cambridge CB2 1EW (UK)
Fax: (+44) 1223-336017
E-mail: mjd13@cam.ac.uk
Prof. Sir J. M. Thomas
The Royal Institution of Great Britain
Davy Faraday Research Laboratory
21 Albermarle Street, London W1X 4BS (UK)

[**] We thank the EPSRC for a studentship to M.D.J. and for their general financial support, ICI for financial support, Newnham College Cambridge for a research fellowship to S.H., and an Oppenheimer Research Fellowship for Y.K.

Supporting information for this article is available on the WWW under http://www.angewandte.org or from the author.

  0044-8249/02/4124-4726 $ 20.00+.50/0